

**FIG. 2.19.** (a)–(d) Changes in global mean tropospheric mixing ratios (ppt) of the most abundant CFCs, HCFCs, HFCs, chlorinated solvents, and brominated gases, calculated from atmospheric measurements made at remote sites in both the NH and SH. [Source: NOAA/ESRL/GMD cooperative air sampling network] (e) Secular changes in atmospheric equivalent chlorine (EECI; ppb). (f) Recent changes in effective equivalent stratospheric chlorine (EESC) observed by the NOAA/GMD global network relative to the secular changes observed in the past. EESC is derived from EECI by adding 3 yr to represent the lag associated with mixing air from the troposphere to the middle stratosphere (updated from Montzka et al. 2003a,b). [Courtesy: S. A. Montzka, J. H. Butler, T. Thompson, D. Mondeel, and J. W. Elkins, NOAA/CMDL]

Increases in HCFCs have slowed notably in recent years. By mid-2005, the Cl in the three most abundant HCFCs amounted to 217 ppt, or 8.0% of all Cl carried by long-lived halocarbons. Mixing ratios of HFC-134a, the most abundant HFC in the global background atmosphere, increased nonlinearly in the 1990s. From 2001 through 2005, however, it has increased in the global troposphere at a fairly constant linear rate of 4.2 ppt yr<sup>-1</sup>. Concern over increases in HFCs is largely due to their efficiency as absorbers of infrared radiation.

The influence of these disparate trends on future levels of stratospheric ozone can be gauged roughly from a sum of Cl and bromine (Br) in long-lived

halocarbons, provided the enhanced efficiency for Br to destroy ozone is considered. This sum is expressed as effective equivalent chlorine (EECI; Fig. 2.19e), and is derived from surface-based measurements. EECI provides an estimate of the O<sub>3</sub>-depleting power of the atmosphere a few years in the future, when air at Earth's surface will have become mixed into the stratosphere.

Observations indicate that the EECI content of the lower atmosphere has declined at a mean rate of 26 ppt yr<sup>-1</sup> since its peak in 1994. Scenarios projecting future halocarbon mixing ratios have been derived elsewhere based upon full compliance with the fully amended and revised Montreal Protocol and our understanding of atmospheric lifetimes of these gases (Montzka et al. 2003b). These analyses suggest that it will take 40–50 years for EECI to decline to the levels present in 1980, before O<sub>3</sub> depletion was first observed. This 1980 level is notable, given that one might expect nearly full recovery of stratospheric ozone once the atmospheric EECI returns to this level. The time frame for O<sub>3</sub> recovery will depend upon other factors as well, such as stratospheric temperatures and atmospheric aerosol loading. Nonetheless, the declines in EECI from 1994 to the present time represent a significant drop in the atmospheric EECI burden. As of 2005, EECI had declined 20% of the way back to the 1980 level (Fig. 2.19f).

Changes in the direct radiative influence of long-lived halocarbons can be estimated from observed changes in atmospheric mixing ratios with knowledge of trace-gas radiative efficiencies. Such an analysis suggests that the direct radiative forcing of these gases was still increasing in 2005, though at a much slower rate than observed from 1970 to 1990.

### 3. GLOBAL OCEANS—J. M. Levy<sup>47</sup> and K. A. Shein<sup>82</sup>, Eds. a. Overview—K. A. Shein<sup>82</sup>

Recent decades have seen a marked increase in our knowledge of the coupled ocean–atmosphere system, although as is discussed, it is only through a number of relatively new or planned ocean-monitoring ac-

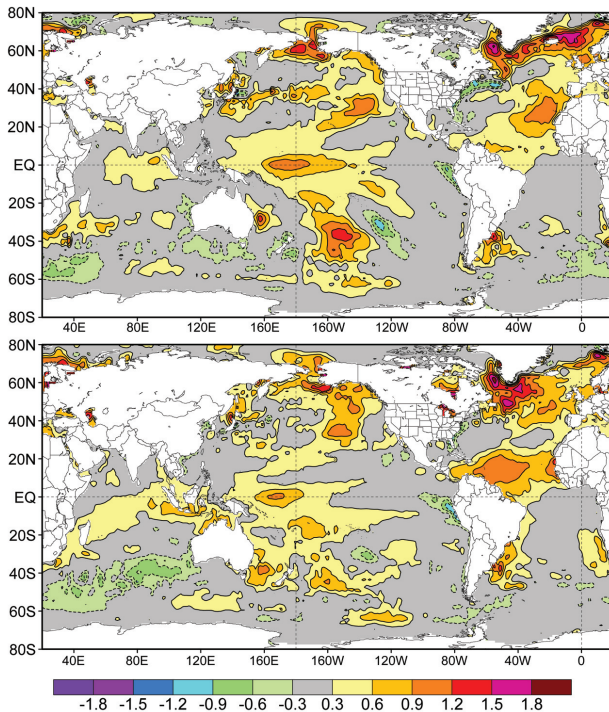


**FIG. 3.1. Annual SST anomalies (°C) for (top) 2004 and (bottom) 2005, computed relative to a 1971–2000 base period.**

tivities that our understanding of these interactions, such as the role of the oceans in the anomalously active 2005 Atlantic tropical storm season, can be improved. Notable characteristics of the oceans in 2005 included above-normal sea surface temperatures, and heat losses that were generally below normal over the global basins. Globally, ocean circulation was near to slightly stronger than normal in 2005, and average sea levels continued their rise for another year. Also, there is preliminary information that anthropogenic carbon inventories may be increasing in the Pacific at about twice the rate of the Atlantic.

**b. Temperature**

**i) SSTs—R. W. Reynolds<sup>69</sup>**

Annually averaged SSTs for both 2004 and 2005 (Fig. 3.1) are derived from monthly fields interpolated from the Reynolds et al. (2002) weekly optimum interpolation (OI) analyses. The analysis uses ship and buoy in situ SST data as well as satellite SST retrievals from the infrared (IR) AVHRR and anomalies are departures from the 1971–2002 base period mean (Xue et al. 2003).

The impression is that the anomalies are primarily positive, and are part of the overall warming trend of global SSTs since 1971. Comparisons of the two years show two important changes: the first in middle lati-

tudes (40°–66°N) and the second in the tropical North Atlantic (0°–30°N). In the midlatitude regions, there is a tendency for the positive anomalies to increase from 2004 to 2005 in the eastern Pacific and western Atlantic. Both regions show an overall warm anomaly for the period of 1995–2005, although variability in the Pacific is less than the Atlantic. There is also evidence of regular summer warming in the Pacific region from 2000 to 2005. This signal is only clearly evident in the Atlantic region in 2003, and is the oceanic response to that summer’s European heat wave.

During 2005, there was a record number of strong Atlantic hurricanes. There has been discussion regarding whether changes in SSTs can imply statistically significant changes in hurricanes (Webster et al. 2005) or not (Trenberth 2005), but all of the reports state that SSTs are not the only variable affecting hurricanes. Because of the changes in the northern tropical Atlantic SSTs from 2004 to 2005, time series are shown for the North Atlantic (10°–30°N) and Gulf of Mexico (Fig. 3.2). The tropical Atlantic region shows overall warm anomalies with irregular variability on 2- to 5-yr periods, which does not strongly correlate with the seasonal cycle or ENSO. However, a relatively strong maximum anomaly occurs in the summer of 2005. The time series from the Gulf of Mexico appears to be noisier without any noticeable signal. Goldenberg et al. (2001) state that local SSTs greater than 26.5°C are needed to generate

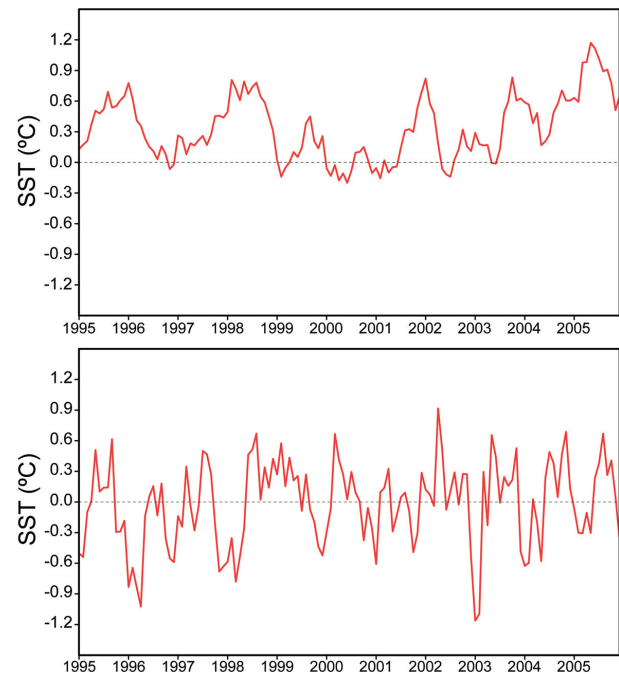


**FIG. 3.2. Time series (January 1995–December 2005) of monthly SST anomalies (°C) for the (top) tropical North Atlantic and (bottom) the Gulf of Mexico.**

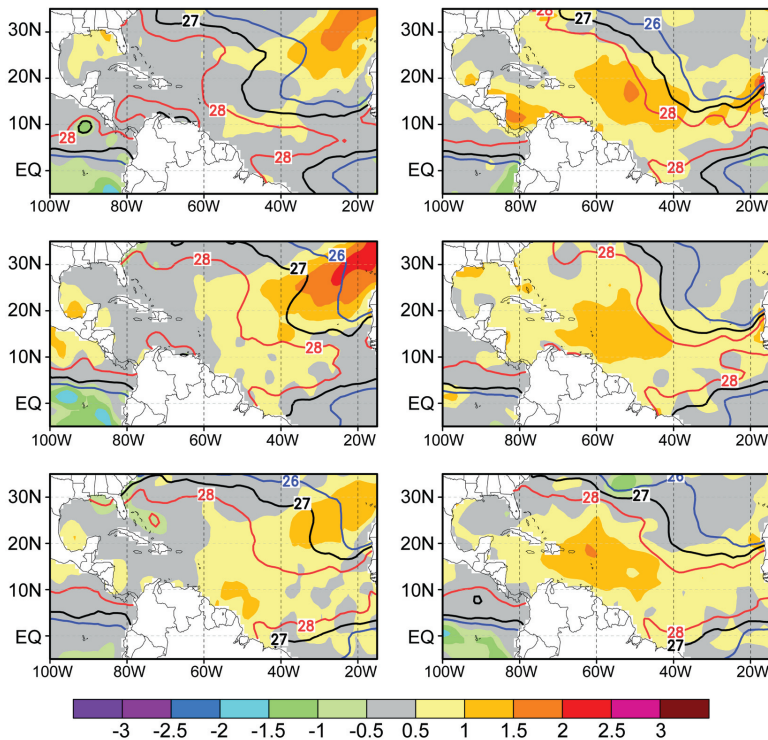


**FIG. 3.3. Tropical monthly SST anomalies (°C) for July, August, and September (left) 2004 and (right) 2005. Contours show the corresponding monthly total (anomaly + climatology) SST isotherms for 26°, 27°, and 28°C.**

hurricanes. A closer examination of the 2004 and 2005 tropical Atlantic anomalies shows that areas exceeding 26.5°C are similar in the corresponding months for 2004 and 2005 (Fig. 3.3). However, the areal extent of SST greater than 28°C is larger in July and August 2005 than in July and August 2004.

ii) **HEAT CONTENT**—G. C. Johnson,<sup>35</sup> J. M. Lyman,<sup>49</sup> and J. K. Willis<sup>93</sup>

Ocean storage and transport of heat and freshwater, and their variations, are intrinsic to many aspects of climate, including El Niño, the North Atlantic Oscillation (NAO), the global water cycle, hurricane seasons, and global change (e.g., Levitus et al. 2005; Hansen et al. 2005). Regional studies of decadal freshwater variability are possible in well-sampled regions like the North Atlantic (e.g., Curry and Mauritzen 2005), but in situ ocean salinity data are too sparse and their reporting is too delayed for a global 2005 perspective of ocean freshwater storage. However, the rapidly maturing Argo Project array of profiling floats measuring temperature and salinity (Roemmich et al. 2004) is remedying this situation.

Here we discuss an estimate of the upper-ocean (0–750 m) heat content anomaly (OHCA) for 2005

produced by combining in situ ocean temperature data and real-time satellite altimetry data collected from 1 January to 31 October 2005 following the techniques of Willis et al. (2004). The 2005 combined OHCA map when compared to a 1993–2002 baseline (Fig. 3.4, top) shows eddy and meander variability down to 100-km mapping scales. There is a great deal of small-scale spatial variability associated with the western boundary currents in every gyre, as well as the Antarctic Circumpolar Current.

Large-scale patterns are also evident in the OHCA. The combined OHCA map for 2005 is high in the subpolar North Atlantic and low in the subtropical North Atlantic, consistent with a decreased strength of the North Atlantic Current. This pattern is probably related to decadal changes in the NAO index (e.g., Curry and McCartney 2001). The NAO index was lower in 2005 than during the baseline period, and has generally trended lower from 1993 through 2005. For the most part, the Tropics in 2005 have

only slightly higher OHCA than average, reflecting the lack of a pronounced El Niño or La Niña in 2005. In 2005, OHCA is high throughout the South Pacific and South Atlantic Oceans in a belt located north of the Antarctic Circumpolar Current. This change may be related to changes in the wind-stress field associated with an increase in the Antarctic Oscillation.

The difference in combined OHCA maps between 2005 and 2004 (Fig. 3.4, bottom) illustrates the large year-to-year variability in ocean heat storage, with changes reaching or exceeding the equivalent of an 80 W m<sup>-2</sup> surface flux. Ocean advection likely plays a large role in many of these changes. Such differences between the two years clearly show the influence of eddies and meanders, but there are also contributions from some of the aforementioned larger-scale patterns in the subtropics and subpolar regions. The decrease of OHCA in the central equatorial Pacific between 2005 and 2004 probably reflects the transition from weak El Niño to more normal conditions. Finally, given the strong 2005 hurricane season and the potential link between hurricane intensity and warm ocean waters (e.g., Emanuel 2005), the large increases in OHCA around Florida and the Gulf of Mexico are also of interest.



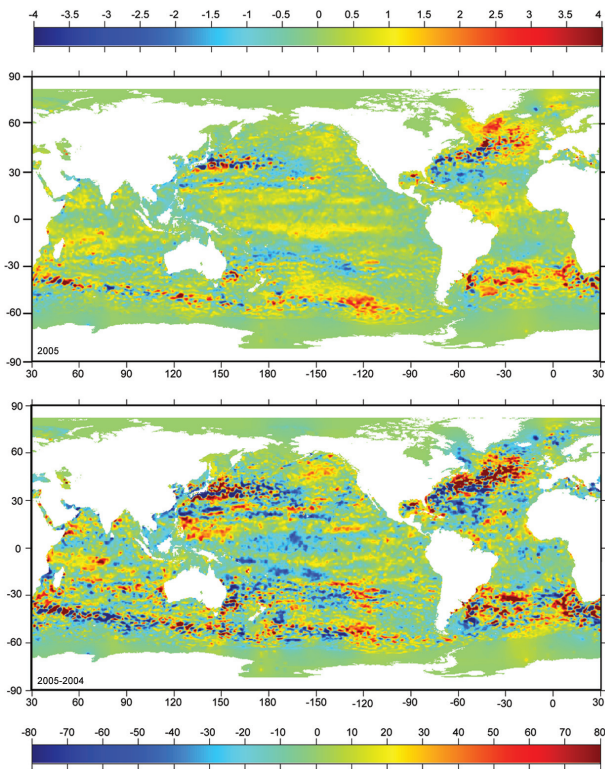


**Fig. 3.4. Combined satellite altimeter and in situ ocean temperature data upper-ocean (0–750 m) heat content anomaly (OHCA) ( $\text{J m}^{-2}$ ) map for (top) 2005 relative to a 1993–2002 base period, following Willis et al. (2004), and (bottom) the difference between 2005 and 2004 OHCA maps expressed as a surface heat flux equivalent ( $\text{W m}^{-2}$ ).**

iii) HEAT FLUXES—L. Yu<sup>96</sup> and R. A. Weller<sup>91</sup>

The oceanic latent heat flux (LHF) is heat energy extracted from the ocean by the evaporation of surface water, and sensible heat flux (SHF) is heat energy transferred by conduction and convection at the air–sea interface. These two fluxes vary with near-sea surface circulation, humidity, and temperature, and influence weather and climate processes. The global change of the two fluxes in 2005 is examined here using daily analyzed fields produced by the Objectively Analyzed Air–Sea Fluxes (OASFlux) project. The resulting flux fields were validated against more than 100 flux buoy measurements acquired by the Woods Hole Oceanographic Institution (WHOI) Upper Ocean Processes group (Moyer and Weller 1997) and by the Pilot Research Moored Array in the Tropical Atlantic (PIRATA) and Tropical Atmosphere Ocean/Triangle Trans-Ocean Buoy Network (TAO/TRITON) moored buoy arrays in the tropical Atlantic and the equatorial Pacific Oceans (Yu et al. 2004).

The 2005 annual mean field of LHF plus SHF over the global oceans (Fig.3.5, top) shows that large

oceanic latent and sensible heat losses occurred over the regions associated with three major Western Boundary Currents (WBCs): the Kuroshio, Gulf Stream, and African Agulhas Currents. In these regions near-surface vertical gradients of humidity and temperature are largest and the wind speeds are greatest in the respective hemisphere’s fall and winter seasons, and the cold season variability of LHF plus SHF dominates the annual mean pattern. On a year-to-year basis, variability of the oceanic heat losses in the three WBC regions is also largest, with magnitudes reaching or exceeding  $40 \text{ W m}^{-2}$ . This is clearly shown from the difference map of the 2004 and 2005 annual mean LHF plus SHF (Fig. 3.5, bottom). Interestingly, the signs of the anomalies associated with different WBC systems are different. For example, the total oceanic heat loss was enhanced (large positive anomalies) from 2004 to 2005 over the Kuroshio region, but reduced (large negative anomalies) over the Gulf Stream region.

Influence of eddy-scale structures is evident in the 2-yr difference map (Fig. 3.4, bottom). Nevertheless, the change in the LHF plus SHF field from 2004 to 2005 is large scale—the anomalies are primarily negative over the global basins, suggesting that the oceanic heat loss was overall reduced in 2005 (Fig. 3.6, top). A persistent, long-term increase in the globally averaged annual mean LHF plus SHF is particularly notable, although that trend appears to have decreased in recent years. It is not clear yet

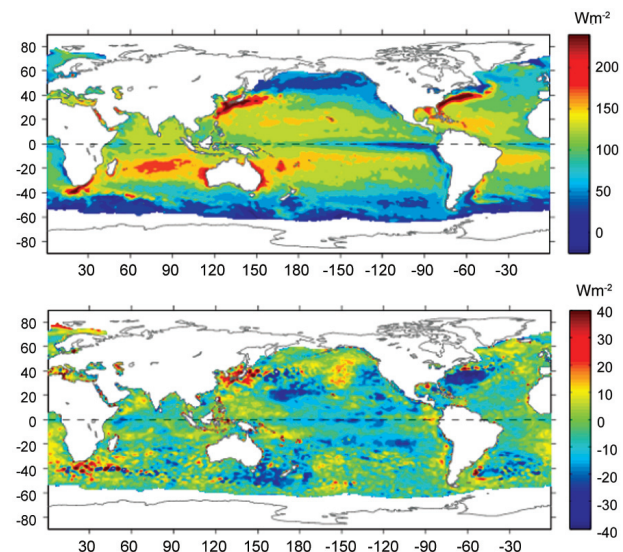


**Fig. 3.5. (top) Annual mean latent plus sensible heat fluxes ( $\text{W m}^{-2}$ ) in 2005. Sign is defined as upward (downward) positive (negative). (bottom) Differences between 2004 and 2005 annual mean latent plus sensible heat fluxes.**



whether or not the reduction in oceanic heat loss for 2005 is a trend change, or merely a short-term anomaly. Additionally, the globally averaged LHF plus SHF has increased by about  $10 \text{ W m}^{-2}$  in the past 20 yr, and the magnitude of the variability is dominated by that of the LHF. The mean SHF value is about one order smaller than that of LHF, and the change in SHF is also small ( $< 2 \text{ W m}^{-2}$ ) over the entire analysis period.

Areal averages of LHF plus SHF variability in the Kuroshio and Gulf Stream regions clearly show a large upward trend in both (Fig. 3.6, bottom). However, unlike the global averages, the regional averages show strong interannual fluctuations. Whereas the upward trend in global averages begins in 1981 (start of the analysis record) and has flattened in recent years, the boundary current regional averages show a trend toward larger values only starting in the early 1990s but remaining positive to the present. Furthermore, the slope of the trend in these two regions is twice as great as that of the global averages. Overall, the regional oceanic heat loss has been enhanced by about  $20 \text{ W m}^{-2}$  over the past two decades.

### c. Circulation

#### 1) SURFACE CURRENTS—R. Lumpkin<sup>48</sup> and G. Goni<sup>30</sup>

Near-surface currents are measured in situ by satellite-tracked drifting buoys and by acoustic point-measuring meters on the Autonomous Temperature Line Acquisition System (ATLAS) moorings. In 2005, the drifter array reached its target goal of 1250 drifters worldwide, becoming the first fully realized component of the Global Ocean Observing System. During 2005, surface currents were well sampled globally, except in the far northern Pacific, the southwest Pacific between  $20^\circ$  and  $40^\circ\text{S}$ ,  $150^\circ\text{E}$  to the date line, the Arabian Basin of the Indian Ocean, and the extreme Southern Ocean south of  $55^\circ\text{S}$ .

A climatology of monthly mean currents was computed from all available drifter observations from 1994 to 2004, using the methodology of Lumpkin and Garraffo (2005). Anomalous currents were calculated with respect to this climatology (Fig. 3.7).

#### (i) Indo-Pacific basins

Annual mean anomalies were most prominent in the tropical Pacific Ocean (Fig. 3.7). Westward anomalies of nearly  $20 \text{ cm s}^{-1}$  were observed on the equator between  $120^\circ\text{W}$  and the date line. Weaker anomalies of  $5\text{--}10 \text{ cm s}^{-1}$  were seen in the North Equatorial Current (NEC) region ( $10^\circ\text{--}20^\circ\text{N}$ ). Drifter observations did not indicate anomalously strong eastward currents in the Kuroshio Extension or North Pacific

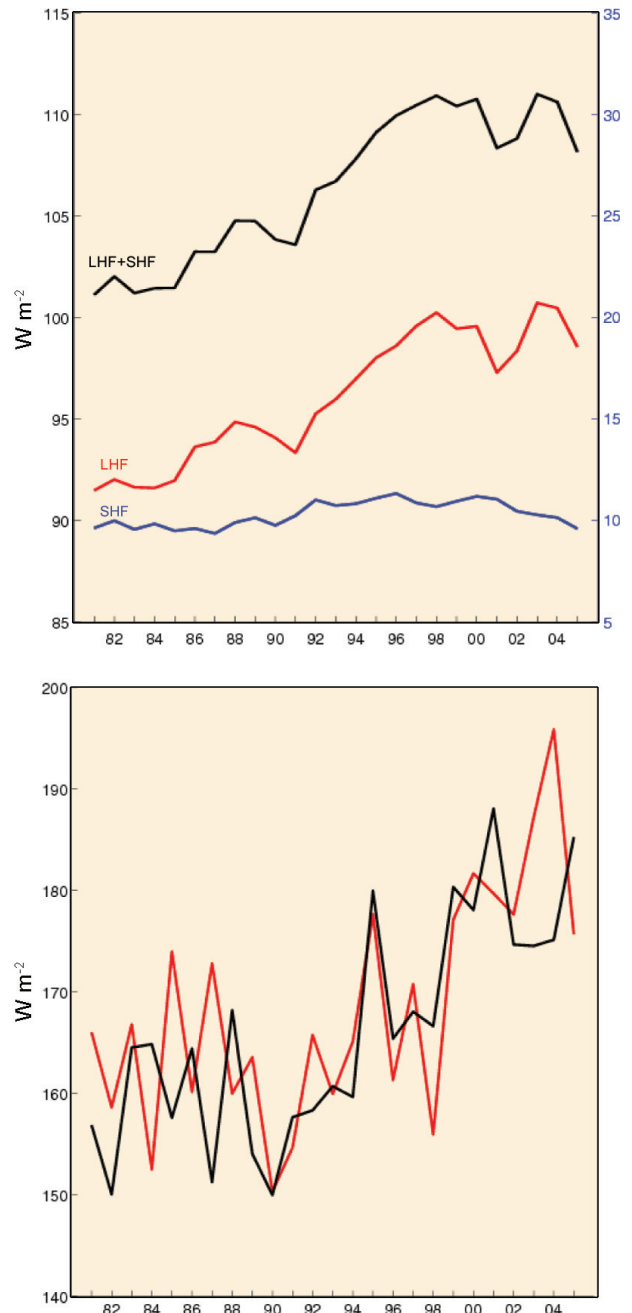


**Fig. 3.6. (top) Year-to-year variations of globally averaged annual mean latent heat flux (red), sensible heat flux (blue), and latent plus sensible heat flux (black). (bottom) Year-to-year variations of the annual mean latent heat plus sensible heat fluxes averaged over the regions of the Gulf Stream [(25°–45°N, 85°–50°W), red] and Kuroshio [(20°–40°N, 120°–150°E), black].**

Current, conflicting with the simple hypothesis of a more-intense-than-average wind-driven gyre.

The strongest intraseasonal anomalies were observed in early 2005 in the western and central tropical Pacific, associated with Kelvin wave activity driven by

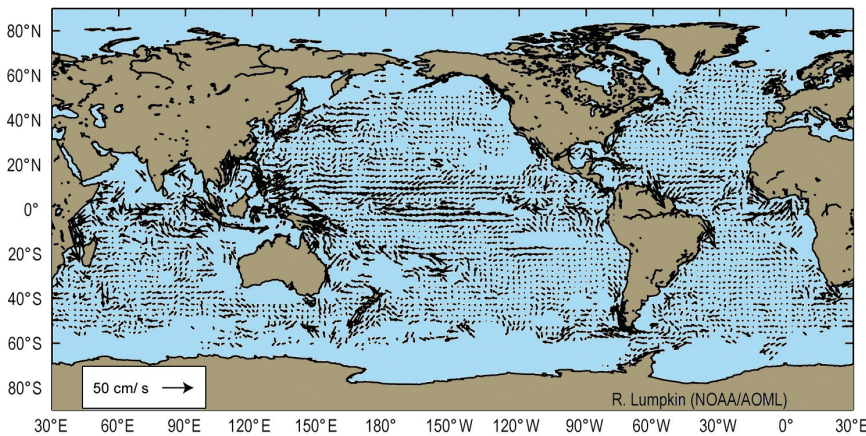


**FIG. 3.7. 2005 mean anomalies ( $\text{cm s}^{-1}$ ) from 1994–2004 surface current climatology.**

intraseasonal (MJO) wind fluctuations (cf. Eisenman et al. 2005). In January (Fig. 3.8), very strong westward anomalies were measured in the northern branch of the South Equatorial Current (nSEC). The nSEC at  $0^{\circ}$ – $5^{\circ}\text{S}$ ,  $160^{\circ}\text{W}$ – $170^{\circ}\text{E}$  was  $80$ – $100 \text{ cm s}^{-1}$  westward, compared to a mean January speed of  $40$ – $60 \text{ cm s}^{-1}$ . During February, a dramatic reversal was seen at  $6^{\circ}$ – $12^{\circ}\text{S}$ ,  $155^{\circ}\text{W}$ – $180^{\circ}$  where several drifters moved eastward at  $50$ – $100 \text{ cm s}^{-1}$ . Drifters suggested the passage of a second Kelvin wave in March and April, when strong westward, then eastward, anomalies were seen west of the date line (Fig. 3.8). This was corroborated by observations at the TAO mooring at  $0^{\circ}$ ,  $170^{\circ}\text{W}$ . The previously noted NEC anomalies were first observed in February. Westward anomalies in the South Equatorial Current (SEC) at  $0^{\circ}$ – $6^{\circ}\text{S}$  appeared in April. Both the NEC and SEC continued to flow anomalously quickly through the remainder of the year.

*(ii) Atlantic Basin*

The North Atlantic subtropical gyre, benchmarked by transport through the Florida Straits and Yucatan Channel, was close to its decadal mean strength during 2005. The Western Boundary Current transport through the Florida Straits, measured by cable voltage, averaged  $31.4 \pm 1.2 \text{ Sv}$  ( $1 \text{ Sv}$  is  $10^6 \text{ m}^3 \text{ s}^{-1}$ ) during 2005 (C. Meinen 2006, personal communication),

the first time, and anomalies here were large, but may reflect a poorly defined climatology for the period of 1994–2004. Thus, it is difficult to tell from these data what role anomalous advection may have played in the development of the unusually large cold tongue during 2005.

*(iii) Southern Ocean*

Drifters did not reveal large-scale anomalies in the strength of the Antarctic Circumpolar Current (Fig. 3.7). From August to December, 18 drifters passed south of Cape Horn. These drifters indicated that the flow entering the Drake Passage was  $8 \pm 9 \text{ cm s}^{-1}$ , much weaker than the mean speed of  $23 \pm 11 \text{ cm s}^{-1}$  here. This anomaly was most prominent during August–September. Four drifters passed through the region during February–May, measuring speeds of  $27 \pm 14 \text{ cm s}^{-1}$

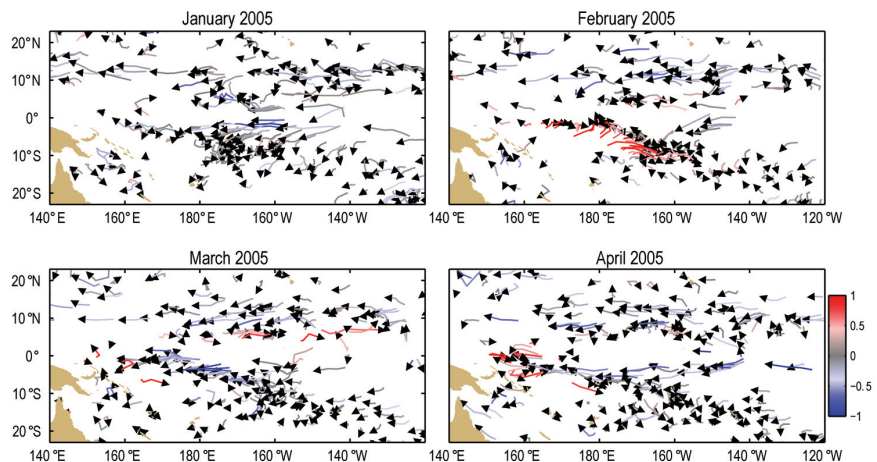


**FIG. 3.8. January–April 2005 drifter trajectories in the tropical Pacific. Arrowheads indicate direction; color indicates zonal speed anomaly ( $\text{m s}^{-1}$ , positive eastward).**

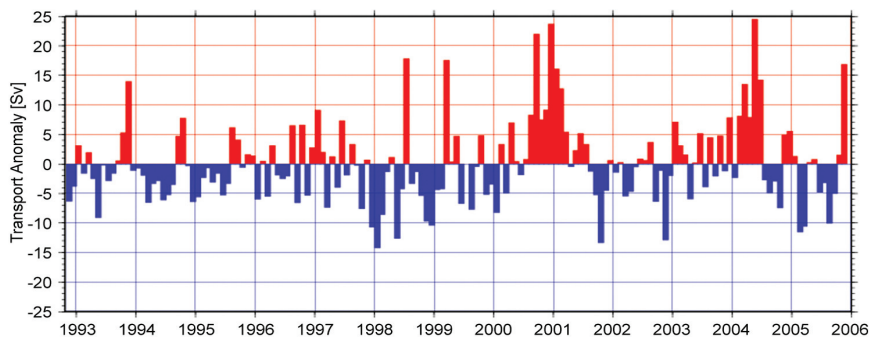


**FIG. 3.9. Monthly geostrophic transport anomalies (Sv) of the Agulhas Current at 28°W derived from satellite altimetry observations.**

(very close to normal). Altimetric estimates of geostrophic transports suggest that the 2005 annual mean of the geostrophic transport remained slightly lower than its historical value, and significantly lower (5–10 Sv) than during 2004 (Fig. 3.9).

ii) THERMOHALINE CIRCULATION—M. O. Baringer<sup>4</sup> and C. S. Meinen<sup>54</sup>

The component of the ocean circulation associated most with variability in heat redistribution is the meridional overturning circulation (MOC), also called the thermohaline circulation. The MOC is a global circulation cell wherein high-latitude surface waters are cooled and become denser, and in certain locations this dense water sinks and flows toward the Tropics. In tropical and subtropical regions around the world these waters warm, become less dense, and return to the surface to flow back toward higher latitudes, while transporting a significant amount of heat. The primary locations where deep convection occurs are in the northern North Atlantic and in the subpolar ocean around Antarctica, while the upwelling of new surface waters is spread broadly around the globe.

Variations in the strength of the overturning circulations are directly related to variations in net poleward heat transport. Current best estimates for the steady-state global mass and heat transport can be found in the analyses of Ganachaud and Wunsch (2003; see also Talley 2003). For example, the North Pacific overturn-

ing cell carries about 0.5 PW northward, but most of this heat transport is associated with water mass transformations in the upper layers of the ocean, while the North Atlantic carries a much larger transport of 1.2 PW northward, most of which is carried in the top-to-bottom MOC system. Typically, it is this deep circulation cell that is described as the MOC, although other oceans and

water masses are important for the redistribution of heat.

The Florida Current contains most of the upper limb of the MOC as it flows through the Florida Straits in the North Atlantic, with a smaller contribution being carried by the Antilles Current east of the Bahamas. Fluctuations in the Florida Current have shown a clear negative correlation with the atmospheric phenomenon known as the NAO, however while the NAO has been trending toward its negative extreme over the past 20 yr, the Florida Current transport shows no such long-term trend through 2005 (Fig. 3.10). The annual mean transport observed in 2005 (31.4 Sv) falls just within the lowest quartile of historical annual mean transports from the cable. However, this transport is well within 1 std dev of the long-term mean of 32.1 Sv, and given the statistical standard error (1 Sv) of the mean for the year, 2005 cannot be considered anomalous in terms of the Florida Current transport.

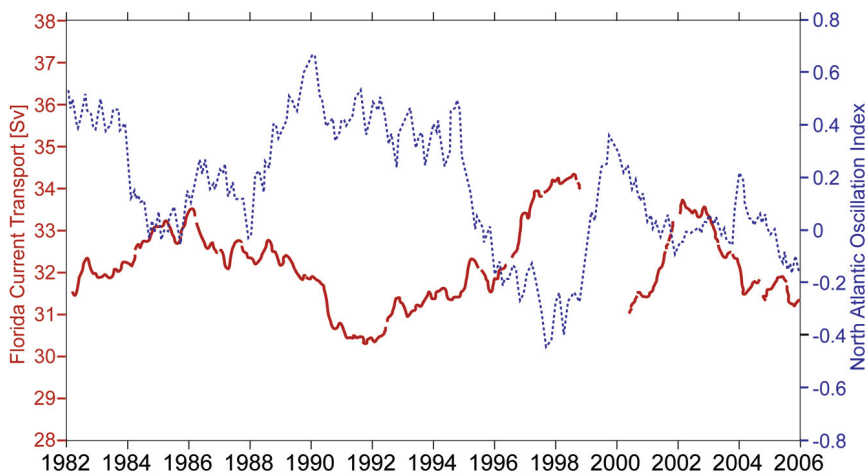


**FIG. 3.10. Florida Current transport (Sv; red solid) as measured by the NOAA-funded submarine cable across the Florida Straits, along with the NAO index (blue dashed) produced by NOAA/NCEP.**



In the near future, a new NOAA-funded system for monitoring the Deep Western Boundary Current coupled with a new international program for monitoring the basin-wide circulation [Meridional Overturning Circulation Heat-Transport and Heat Flux Array (MOCHA)] will allow for a greater degree of certainty in statements regarding variations in the integrated, basin-wide MOC circulations and the time scales on which they vary. Bryden et al. (2005), postulated a 30% reduction in the MOC transport between the 1950s and the present day; however, that analysis was based on a very limited dataset. Other data over the past few decades, such as the moored observations of the Deep Western Boundary Current at the southeast Newfoundland Rise in the early 1990s and early 2000s showed no indication of such a significant trend in the MOC (F. Schott 2005, personal communication). In contrast, Koltermann et al. (1999) showed the large variability of the MOC that they concluded was related to the strength of Labrador Sea Water production with larger (smaller) MOC transport corresponding to less (more) Labrador Sea Water export. More recently, these data have been reanalyzed to formally test the hypothesis that the MOC circulation was steady. Lumpkin et al. (2006, manuscript submitted to *J. Mar. Res.*) found that a steady MOC over the same time period could not be ruled out, based on the uncertainty in determining the barotropic circulation. Also, if Bryden et al. (2005) are correct in that the thermohaline circulation has been reduced over the past 50 yr by 30%, this represents a much higher rate of change than that

predicted in coupled climate model simulations (e.g., Schmittner et al. 2005).

Changes in heat transport on the order of 30%, such as that postulated by Bryden et al. (2005), could have substantial impacts on climate, and time series observations are clearly necessary in order to put one-time hydrographic sections in temporal context. The programs in place in 2005 are an excellent first step toward the development of an integrated measurement system, including repeated hydrographic sections and moored observations that can play a significant role in measuring and monitoring the MOC system over a broader range of locations than would be feasible with moored instrumentation alone. However, much work remains before it will be possible to state that the Atlantic MOC system, much less the global overturning circulation system, is truly being monitored.

d. *Sea level*—M. A. Merrifield,<sup>56</sup> S. Gill,<sup>26</sup> and G. T. Mitchum<sup>57</sup>

Data on sea level were obtained from both tide gauges and satellite altimetry [Ocean Topography Experiment (TOPEX)/Poseidon/Jason]. Tide gauges have long observed sea level, and these instruments still provide the long-term context for understanding climate variations. Since 1992, however, satellite altimetry has provided global views of the sea surface height field. Sea level anomalies in 2005 were computed relative to 1993–2001 mean values (Fig. 3.11). Coastal and island sea level deviations, as measured by tide gauges, were generally consistent with the deep ocean patterns measured by satellite altimeters.

A notable exception was the east coast of North America, where coastal tide gauge sea levels were higher than normal, whereas nearby ocean values from altimetry were lower than normal.

The deviations shown in Fig. 3.11 were above average over most of the global ocean. Since at least 1993 (the time span of TOPEX/Poseidon/Jason altimeter measurements) global sea levels have been rising at a linear rate of  $2.9 \pm 0.4 \text{ mm yr}^{-1}$  (Leuliette et al. 2004; Cazenave and Nerem 2004; see also information online at <http://sealevel.colorado.edu/>). The general increase in globally averaged sea level during 2005 was consistent with this longer trend. At any particular point, however, the rate of sea level change can be very different from the globally aver-

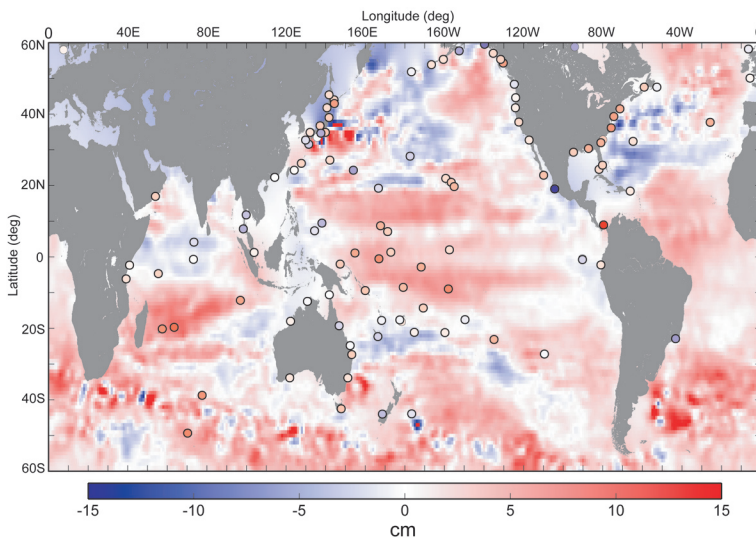


**FIG. 3.11. Deviation of 2005 annual average sea level (cm) from 1993 to 2001 mean, as measured by (colored shading) satellite altimeter and (filled circles) tide gauges. [Source: University of Hawaii Sea Level Center]**

aged rate. A notable example is along the coasts of North America, where sea level has fallen in recent years. In the North Pacific, this is presumably associated with a trend in equatorward winds near the coast, which favor upwelling. Recent sea level trends appear to be determined by the polarity of the Pacific Decadal Oscillation (Mantua et al. 1997; Cummins et al. 2005; see information online at <http://tao.atmos.washington.edu/pdo/>), and it seems likely that the North Pacific sea level trend pattern will reverse sign, resulting in rising sea levels near the North American coast.

Other regional patterns also are evident. In general, levels were higher than average in the Tropics and the Southern Hemisphere. Regions of lower-than-average sea level occurred in the midlatitude North Atlantic, the North Pacific, the tropical Indian Ocean, and off the east and west coasts of Australia. In many instances, the sea level deviations can be linked directly to anomalous surface winds (Fig. 3.12). A striking example is a cyclonic wind anomaly centered over the North Atlantic. This anomaly corresponds to a weakening of the Bermuda high, and possibly to a corresponding weakening of the subtropical oceanic gyre. This would account for the aforementioned lowered sea level in the open ocean, and the higher-than-average tide gauge sea levels along the North American coast.

Relative to the previous year, 2005 saw a noticeable increase in sea level in the region of the western tropical Pacific north of the equator and east of the Philippines. This pattern developed in response to the increased local anticyclonic wind forcing in 2005 relative to 2004. Otherwise, sea level changes in the tropical oceans were generally weak, consistent with the relatively weak ENSO variability experienced in 2005 (see section 4b).

In addition to these large-scale, low-frequency patterns, extreme sea levels were also examined. NOAA has developed a new exceedance probability product from long-term tide station records using a generalized extreme value analysis approach (Zervas et al. 2005). The remarkably active hurricane season of 2005, in terms of number and severity of storms, produced unusually extreme water levels on the east and Gulf coasts of the United States. The eastern Pacific was also subject to extreme water levels associated with several tropical cyclones (see section 4c).

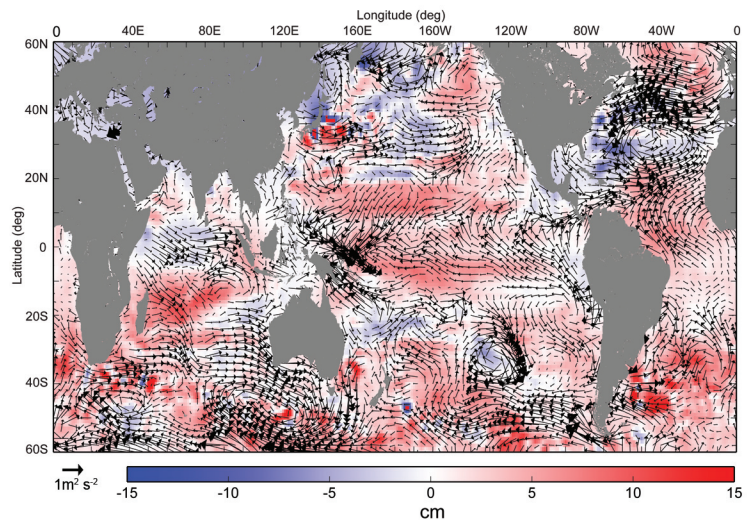


**FIG. 3.12.** Same as Fig. 3.11, excluding tide gauge deviations, and including the 2005 deviation of surface winds ( $\text{m}^2 \text{s}^{-2}$ ). [Source: NCEP]

e. *Ocean carbon*—C. L. Sabine,<sup>79</sup> R. A. Feely,<sup>22</sup> and R. Wanninkhof<sup>88</sup>

The paucity of carbon measurements in the ocean currently impedes our ability to generate annual assessments of global anomalies. However, our understanding of the global ocean carbon cycle has greatly improved over the last decade based on accumulated data and modeling activities. Our best estimates of the current distributions of natural and anthropogenic carbon in the ocean stem from the collaborative efforts of two international programs—the World Ocean Circulation Experiment (WOCE) and the Joint Global Ocean Flux Study (JGOFS)—to conduct an extensive survey of the chemical and physical properties of the global ocean in the 1990s (Feely et al. 2001; Wallace 2001). An analysis of more than 70,000 carbon measurements from this survey found that the ocean accumulated approximately 118 Pg of carbon between 1800 and 1994 (Sabine et al. 2004). This accumulation accounts for 48% of the  $\text{CO}_2$  released from fossil fuel combustion over this same time period.

Because there were no ocean carbon measurements prior to the mid-1800s, the anthropogenic  $\text{CO}_2$  component of the total dissolved inorganic carbon (DIC) concentration was estimated using a back-calculation technique based on current understanding of the physical and biological contributions to the measured DIC (Gruber et al. 1996; Sabine et al. 2004). As a consequence, it is implicitly assumed that the ocean circulation and biological processes were in steady state over the industrial era. Although this work provided our best assessment of the state of the

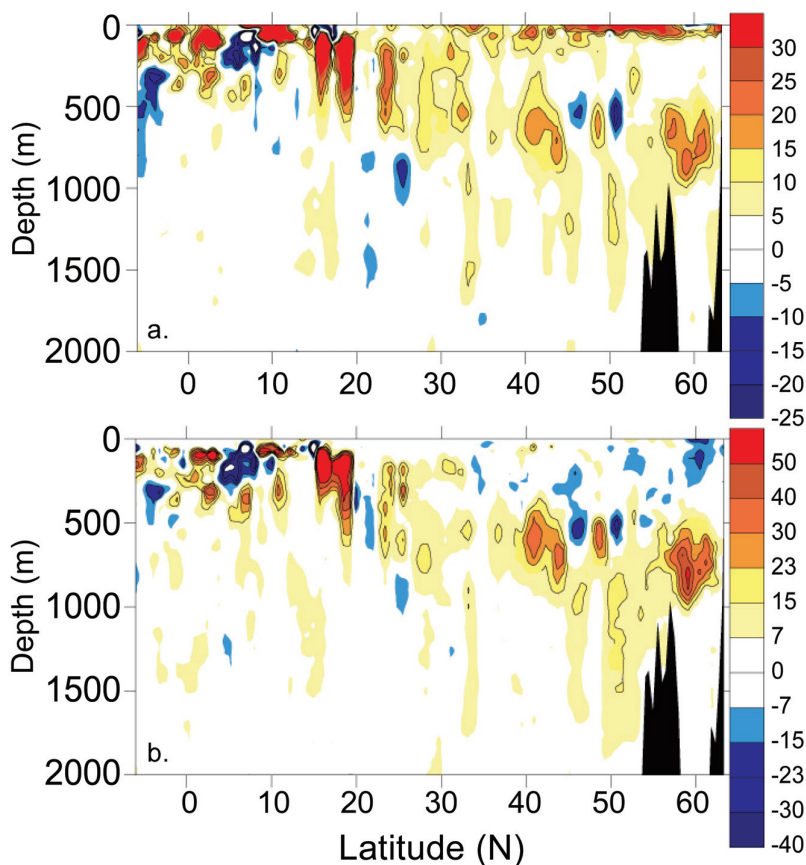


**FIG. 3.13. Changes in (a) DIC ( $\mu\text{mol kg}^{-1}$ ) and (b) AOU ( $\mu\text{mol kg}^{-1}$ ) in the upper 2000 m between the 2003 and the 1993 occupations of A16N. Positive values are an increase in concentrations between 1993 and 2003 (modified from Feely et al. 2005).**

ocean in the mid-1990s, these studies are unable to establish temporal and spatial scales of variability, or the temporal evolution of the ocean carbon cycle.

To address questions of decadal variability and temporal evolution, the U.S. Climate Variability and Predictability (CLIVAR)  $\text{CO}_2$  Repeat Hydrography Program has identified 19 hydrographic sections distributed around the global ocean that will be re-occupied every 5–10 years. The program began in 2003 with three cruises in the North Atlantic that were repeats of cruises in the 1990s. Each year one to three cruises are run in different locations with a goal of completing the first global resurvey by 2012. In 2005, cruises were run in the South Atlantic and South Pacific Oceans, but these data will take several years to finalize and thoroughly examine.

Analysis of the initial repeat lines over this past year has indicated that several biogeochemical parameters are changing with time (Feely et al. 2005). For example, changes of  $-10$  to  $+30 \mu\text{mol kg}^{-1}$  of DIC have been observed in the upper 1000 m of the water

column between the 1993 and 2003 occupations of a track designated as A16N along  $25^\circ\text{W}$  in the North Atlantic (Fig. 3.13a). Although the magnitude of the changes is not surprising, the patchiness of the changes was not expected. More surprising is the fact that there have been similar changes in the apparent oxygen utilization (AOU) of the waters (a measure of the decomposition of organic matter in the ocean), indicating significant changes in the organic matter cycling over the last decade that was previously believed to be in steady state (Fig. 3.13b). The complicated patterns of these changes clearly show that carbon is being influenced by more than simple secular increases in atmospheric  $\text{CO}_2$ . In some cases changes in circulation and organic matter cycling may be masking anthropogenic changes, and in other cases these changes may enhance the apparent ocean carbon uptake.

Another intriguing preliminary finding from a comparison of a 2004 cruise in the North Pacific to the aforementioned North Atlantic results is that anthropogenic carbon inventories may be increasing in the Pacific at about twice the rate of the Atlantic over the last 10 years (Feely et al. 2005). This is in contrast to the long-term anthropogenic  $\text{CO}_2$  inventory that shows larger column inventories in the North Atlantic. The interpretation of these recent findings may lie in understanding the effects of climate modes like the NAO or the Pacific Decadal Oscillation (PDO) on the decadal-scale circulation. These results also point to the need for improved approaches for isolating the anthropogenic and natural components of the observed variability.

#### **4. THE TROPICS**—H. J. DIAMOND<sup>19</sup> AND K. A. SHEIN,<sup>82</sup> Eds.

##### *a. Overview*—H. J. Diamond<sup>19</sup>

This Tropics section consists of global input on two primary topics: 1) ENSO and the tropical Pacific, including ENSO seasonal variability, and 2) tropical cyclone activity for the 2005 season in the following seven basins: the Atlantic, northeast Pacific, northwest Pacific, North and South Indian,